Journal of Marine Research, 73, 123–140, 2015

Intertidal percolation through beach sands as a source of ^{224,223}Ra to Long Island Sound, New York, and Connecticut, United States

by Henry Bokuniewicz[1], J. Kirk Cochran[2], Jordi Garcia-Orellana[3,4], Valenti Rodellas[4], John Wallace Daniel[5], and Christina Heilbrun[6]

ABSTRACT

Along tidal coasts, seawater circulated through the intertidal beach contributes to submarine groundwater discharge (SGD) and its associated geochemical signature. The short-lived radium isotopes, ^{223}Ra (half-life = 11.4 d) and ^{224}Ra (half-life = 3.66 d), were used to quantify this component of SGD in a large estuary, Long Island Sound (LIS), New York, United States. The tide is semidiurnal with a range of approximately 2 m. Concentrations in beach pore waters ranged from 97 to 678 disintegrations per minute (dpm) ^{224}Ra 100 L^{-1}, whereas concentrations in open coastal waters ranged from approximately 12 to 69 dpm ^{224}Ra 100 L^{-1}. A simple model based on ingrowth of ^{224}Ra in the pore water of the beach sands was used to determine residence times of 0.6 to 2.5 d for water in the intertidal beach. Both ^{223}Ra and ^{224}Ra showed decreasing gradients and concentration in an offshore transect away from the beach face in Smithtown Bay, whereas the long-lived radium isotopes, ^{228}Ra (half-life = 5.75 y) and ^{226}Ra (half-life = 1,600 y), showed no significant gradients. Based on the ^{224}Ra gradient, the flux across the LIS shoreline was estimated to be 1.79×10^8 dpm m^{-1} y^{-1}. The ^{224}Ra inventories in two zones, 0–50 m and 0–100 m offshore, were used to estimate total SGD fluxes of 3.1×10^{10} to 6.6×10^{10} m^3 y^{-1} of intertidal seawater to the nearshore of LIS. Comparison of this estimate with hydrodynamic models of fresh groundwater flow in the adjacent coastal aquifer suggests that less than 1% of the SGD is freshwater.

Keywords: Submarine groundwater discharge, radium geotracers, beach hydrogeology

1. School of Marine and Atmospheric Sciences, State University of New York, Stony Brook, NY 11794-5000. Corresponding author: ***e-mail: Henry.bokuniewicz@stonybrook.edu***

2. School of Marine and Atmospheric Sciences, State University of New York, Stony Brook, NY 11794-5000. ***e-mail: kirk.cochran@stonybrook.edu***

3. Departament de Física, Universitat Autònoma de Barcelona, E-08193 Bellaterra, Spain. ***e-mail: jordi.garcia@uab.cat***

4. Institut de CiènciaiTecnologiaAmbientals (ICTA), Universitat Autònoma de Barcelona, E-08193 Bellaterra, Spain. ***e-mail: valenti.rodellas@uab.cat***

5. School of Marine and Atmospheric Sciences, State University of New York, Stony Brook, NY 11794-5000. ***e-mail: jwrdaniel@gmail.com***

6. School of Marine and Atmospheric Sciences, State University of New York, Stony Brook, NY 11794-5000. ***e-mail: Christina.Heilburn@stonybrook.edu***

1. Introduction

Although definitions vary, here we adopt the broad sense of the term "submarine groundwater discharge" (SGD) proposed by Burnett et al. (2003) as any net volume flux of sediment pore water up across the sediment-water interface. This includes not only meteoric water from the terrestrial aquifer but also a portion of seawater circulated through the coastal aquifer (Taniguchi et al. 2002). Often, 90% or more of SGD is composed of circulated seawater (Li et al. 1999). Seawater can be incorporated into SGD in several ways (e.g., Xin et al. 2010). The dispersion of salt across the Ghyben-Herzberg saltwater–freshwater interface at depth in the aquifer draws saline groundwater into the upward seepage from the freshwater lens (e.g., Smith 2004). The magnitude of this circulation depends on the terrestrial hydraulic gradient, the length of the interface, and the magnitude of hydraulic dispersion to distribute salt across the saltwater–freshwater boundary. Such dispersion occurs over a horizontal scale of up to kilometers, but a vertical scale of, often, only a few meters along a saltwater–freshwater interface. Circulation also occurs right at the sediment–water interface in subtidal sediments. At the seafloor, various mechanisms, like gravitational convection or bioirrigation, allow the overlying saltwater to be dispersed downward into the upward-flowing SGD (Rapaglia and Bokuniewicz 2009). This dispersion occurs over a horizontal scale of up to kilometers along the seafloor, but over a vertical scale of mere decimeters depending on the physical or biological processes of vertical dispersion. In the intertidal zone, there is a third type of circulation in what has been referred to as the "upper salinity plume" (e.g., Urish and McKenna 2004; Vandenbohede and Lebbe 2006; Brovelli, Mao, and Barry 2007; Santos et al. 2009). The upper salinity plume is created by the percolation of seawater into the beach during periodic inundation due to tides and waves (Turner and Masselink 1998; Austin and Masselink 2006). Modeling suggests that, where the tidal range exceeds 2 m, the upper salinity plume may extend to a depth of a few meters under the intertidal beach (Smith 2004; Robinson, Li, and Barry 2007; Abarca et al. 2013). Circulated seawater in the upper salinity plume may have residence times up to a week or two, but the residence time should be expected to decrease in highly permeable beaches and under high-energy wave pumping and high tidal pumping during spring tides. Our study area is characterized by small waves and steep beaches, but a fairly large tidal range. Wave setup is small, but seawater introduced onto the unsaturated beach by wave up-swash is distributed across a wider intertidal zone by the tidal excursion.

SGD is, therefore, a mixture of components each of which has a different biogeochemical history. Different flow paths will expose parcels of groundwater to different sequences of oxygen concentrations, pH levels, temperatures, and metabolites. This blended SGD is known to be an important source of nutrients (e.g., Krest et al. 2000), trace metals (e.g., Windom et al. 2006), or radionuclides (e.g., Garcia-Orellana et al. 2013) to the coastal ocean. It is well documented that SGD plays an important role in many coastal biochemical cycles (e.g., Valiela et al. 1990; Slomp and Van Cappellen 2004).

In coastal tidal environments, SGD may be largely composed of seawater circulated through beach sand. The intertidal zone represents a key environment of nutrient recycling

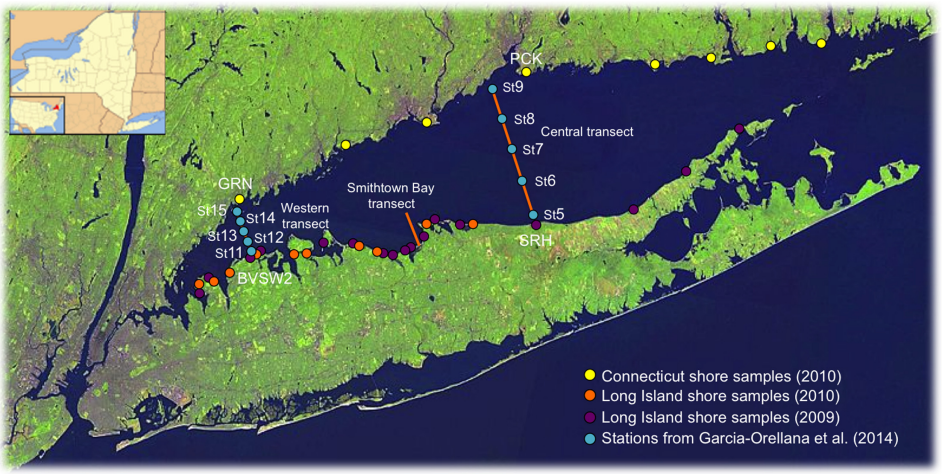

Figure 1. Sample locations in Long Island Sound and along the shore. BV, Bayville, New York; GRN, Greenwich, Connecticut; PCK, Peck Avenue, West Haven, Connecticut; SRH, Shoreham, New York; St, station. BVSW2, Bayville Seawater Sample #2 (see Table 1).

and subsequent discharge via SGD (e.g., Ullman et al. 2003; Boehm et al. 2006; Hays and Ullman 2007; Deborde et al. 2008; Loveless and Oldham 2010). Anschutz et al. (2009) demonstrated that beaches, often thought of as "geochemical deserts" because of the low concentrations of organic matter, can act as effective biogeochemical reactors as infiltrating water with its burden of reactive carbon circulates through the sand.

Here we use the natural radionuclides ^{224}Ra (half-life = 3.66 d) and ^{223}Ra (half-life = 11.4 d) as tracers for this intertidal component of SGD in Long Island Sound (LIS), New York, United States. Both radium isotopes are produced by the decay of thorium parents within or on the surfaces of the beach sands. A fraction of the nascent radium atoms are recoiled to the pore water during production. A rising tide carries wave swash onto an undersaturated beach face. As seawater percolates through the beach face, radium accumulated in pore waters can mix with radium transported in fresh groundwater from inland and leaves the sediment via SGD (e.g., Urish and McKenna 2004). This process should produce elevated activities of ^{224}Ra (and ^{223}Ra) in the waters immediately offshore. Indeed, previous work has shown such patterns of ^{224}Ra in nearshore waters. For example, Torgersen et al. (1996, p. 1550), in measurements of ^{224}Ra in surface transects across LIS, concluded that the "distribution of surface ^{224}Ra along the sound's axial transect could only arise from sources more shoreward than the transect endpoints with minimal water column production." Similarly, recent measurements of ^{224}Ra in transverse transects across the sound showed that activities were elevated relative to stations in the central sound and suggested a significant coastal input of ^{224}Ra, especially along shorelines composed of sandy sediments (Fig. 1; Garcia-Orellana et al. 2014).

2. Setting

LIS is a large estuary located between Long Island, New York, and Connecticut (Fig. 1). It is approximately 93 km long and 34 km wide with a salinity ranging between 23 and 31. The reduced salinity is mainly attributable to fluvial discharge, but the seepage of fresh groundwater particularly from the Long Island shoreline also contributes (Monti and Scorca 2003). The amount of fresh groundwater flowing under the shoreline through the coastal aquifer in Nassau and Suffolk counties has been estimated from a groundwater-flow model to be 0.034×10^{10} m^3 y^{-1}(Monti and Scorca 2003).

In eastern LIS, the tidal range is less than 1 m, but in the central and western sound, the tidal range can exceed 2 m. Waves in LIS are generated by local winds alone as fetches are limited from most directions. As a result, the relatively protected shorelines of LIS are not subject to significant waves except during storms (e.g., during a nor'easter when the winds blow along the axis of the sound). Hourly wave observations from the central sound in 2002 and 2003 (http://sounddata.uconn.edu/) recorded that the average wave height was 0.48 m, ranging up to 2.9 m. Wave periods were between 6.6 and 2.2 s, averaging 3.0 s.

The sound's southern (New York) shoreline is predominantly composed of coarse-grained, permeable sand. The northern (Connecticut) shoreline is rocky with pocket beaches. Given the fairly large tidal range and the relatively high permeability of the beach, seawater circulation through the upper salinity plume might be expected to make an important contribution to SGD.

Smithtown Bay is one location of particular interest on the south shore of LIS because water quality there is regularly impaired by localized hypoxia. The mean tidal range in Smithtown Bay is 2.1 m. Wave heights in the sound exceeded a tidal range of 2.1 m only 0.6% of the time and were less than 0.3 m 44% of the time. The intertidal beaches here have a median grain size ranging between 2 and 3 mm (Davies, Axelrod, and O'Connor 1972). Beach slopes measured at two locations were 1:6 and 1:9 generating a horizontal intertidal zone between 13 and 19 m wide. The average wave excursion would be approximately 23% of the total tidal excursion.

Although the surrounding bottom waters outside of Smithtown Bay have remained oxygenated, hypoxia (dissolved oxygen <3.0 mg L^{-1}) has recurred almost every year in Smithtown Bay since at least 1991. Hypoxia is generally recognized to be attributable to microbial oxygen consumption of excess organic matter resulting from a surplus of nitrogen loadings from both point and nonpoint sources into LIS (Welsh and Eller 1991). This occurs, in part, because the bay waters are partially isolated from the sound by a tidally generated headland eddy (Bowman and Esaias 1977; Bauer 2012), which increases the residence time of water in Smithtown Bay. Nonpoint sources of nutrients, like SGD, may be especially important in the bay where there is little stream discharge and the only point source discharging into Smithtown Bay is Kings Park Sewage Treatment Plant. The Kings Park Sewage Treatment Plant is a relatively small facility that discharges only 0.4×10^6 m^3 y^{-1}. Before 2010, the plant released 8.1 t N y^{-1} (R. L. Swanson, 2015, Stony Brook University, personal

communication). After the plant was upgraded in 2010, nitrogen release was reduced to 2.4 t N y^{-1}.

3. Methods

Samples were taken along both the north shore and the south shore of LIS as well as in Smithtown Bay itself. In Smithtown Bay, 12 surface samples (40–60 L) were collected along a transect extending from shore to 4 km offshore (Fig. 1). Temperature and salinity were measured using a YSI 556 Multiple Probe System conductivity, temperature, and depth (CTD) device. Samples were obtained with a submersible pump at a depth of approximately 0.5 m and filtered from triple-rinsed plastic carboys through cartridges containing approximately 15 g radium-adsorptive MnO_2-impregnated acrylic fiber (Mn-fiber). Untreated fiber was used as a prefilter to eliminate particles. The ^{223}Ra and ^{224}Ra were quantified using a delayed coincidence counting detector (Moore and Arnold 1996; Garcia-Solsona et al. 2008). A few of the samples from the transect were also analyzed for long-lived radium isotopes (^{226}Ra, half-life = 1,600 y; ^{228}Ra, half-life = 5.75 y). Following completion of ^{223,224}Ra analyses, radium was leached off the Mn-fiber and coprecipitated with $BaSO_4$, which was counted in a well germanium gamma detector. The 352 keV ^{214}Pb and 911 keV ^{228}Ac gamma peaks were used to quantify ^{226}Ra and ^{228}Ra, respectively. NIST Standard Reference Material 4350B was used for calibration of the gamma peaks.

Along the shoreline of LIS, surface seawater (40 L samples taken at 0.1 m depth) was also sampled at 39 coastal locations (Table 1; Fig. 1) during ebb tide, between mid- and low tide. Temperature and salinity measurements were recorded using a YSI 556 Multiple Probe System CTD (Table 1). At 19 of these locations, 5–10 L of pore water was taken from shallow pits (∼30 cm deep) dug into the subaerial beach at low tide closest to the low-tide shoreline. Pore-water sampling was conducted at four sites along the north shore (Connecticut) of LIS and 15 sites along the Long Island (New York) south shore of LIS, including the shoreline of Smithtown Bay, New York (Fig. 1; Table 1). Both surface- and pore-water samples were analyzed for ^{224}Ra only, using the method described previously.

4. Results

Concentration of ^{224}Ra in the surface waters at the beach sites ranged from 12 to 69 disintegrations per minute (dpm) 100 L^{-1} (Table 1). The ^{224}Ra concentrations in surface waters at the beach were comparable to those of LIS water column stations closest to the shore. For example, the concentration of ^{224}Ra in surface waters was 20.2 dpm 100 L^{-1}on the New York shore, specifically Shoreham, New York (40.9670 N, 72.8538 W; SRH in Table 1; Fig. 2). The open-water station 2.2 km to the north had ^{224}Ra concentrations of 27.5 dpm 100 L^{-1} (Garcia-Orellana et al. 2014; St5 in Fig. 2).

Pore-water ^{224}Ra activities along the Long Island shore were between 4 and 27 times higher than surface water adjacent to the beach and ranged from 97 to 678 dpm 100 L^{-1}, averaging 313 dpm 100 L^{-1} (Fig. 3; Table 1). The maximum and minimum values were

Table 1. Nearshore and pore water ^{224}Ra concentrations (disintegrations per minute [dpm] 100 L^{-1}).

Station ID	Location	State	Latitude (N)	Longitude (W)	Date sampled	Salinity	Temperature (°C)	^{224}Ra (dpm 100 L^{-1})
Nearshore water								
ASH	Asharoken (aka HBT)	NY	40.9286	−73.4034	22/05/09	25.7	18.9	34.3 ± 1.3
BTR	Belleterre	NY	40.9641	−73.0489	28/05/09	25.1	12.9	55.1 ± 3.8
BVSW1	Bayville	NY	40.9088	−73.5929	18/05/09	24.4	15.2	17.6 ± 0.9
BVSW2	Bayville	NY	40.9153	−73.5651	18/05/09	24.9	14.1	24.6 ± 1.6
CDB	Cedar Beach	NY	40.9654	−73.0311	10/06/10	25.7	18.6	34.5 ± 3.5
CRM	Crab Meadow Beach	NY	40.9299	−73.3249	18/06/10	23.6	19.5	50.1 ± 5.6
GRN	Greenwich	CT	41.011	−73.6223	14/09/10	27.6	22.3	38.5 ± 3.6
HBT	Hobart Beach	NY	40.9285	−73.4034	18/06/10	25.7	20	69.2 ± 7.0
HRK	Harkness	CT	41.3004	−72.1162	13/09/10	30.4	19.2	41.8 ± 4.2
HSP	Hammonaset	CT	41.2595	−72.5573	13/09/10	28.5	20	40.2 ± 4.1
HVY	Harvey's Beach	CT	41.2737	−72.3952	13/09/10	28.8	19.7	40.1 ± 2.7
LB	Smithtown, Long Beach	NY	40.9196	−73.1795	9/05/09	26.1	15.9	53.6 ± 2.9
LRD	Lordship Beach	CT	41.1475	−73.1294	14/09/10	27.8	19.2	57.7 ± 3.4
LYD	Lloyd Harbor	NY	40.9153	−73.4512	22/07/10	25.8	26.5	54.9 ± 5.4
NAV	Webb Institute	NY	40.8833	−73.648	22/06/10	24.6	20.4	20.4 ± 2.3
NOP	Northport (aka CRM)	NY	40.9297	−73.3270	26/05/09	13.7	24.9	63.8 ± 4.9
NTH	Northville	NY	40.9878	−72.6169	16/06/09	25	15.8	26.6 ± 1.3
OFP	Old Field Point	NY	40.9771	−73.1196	10/06/10	25.4	20	15.5 ± 1.8
OLD	Old Field	NY	40.9663	−73.1507	25/05/09	26.2	14.4	32.4 ± 2.4
ORI	Orient	NY	41.1398	−72.3207	16/06/09	27.6	15.4	65.1 ± 1.9
PCK	Peck Avenue, West Haven	CT	41.2585	−72.9402	14/09/10	27.5	18.9	37.1 ± 3.7
PJ PRT	Port Jefferson	NY	40.9499	−73.0701	1/06/09	25.3	14.7	20.5 ± 1.5
PJ IN	Port Jefferson	NY	40.9687	−73.0909	1/06/09	25.8	14.7	12.3 ± 1.0
PJ HB	Port Jefferson	NY	40.9593	−73.0803	1/06/09	25.8	15.3	20.4 ± 1.5
PW	Port Washington, Sands Beach Association	NY	40.8364	−73.7296	9/05/09	24.5	14.9	11.9 ± 0.7
PW	Port Washington, Sands Beach Association	NY	40.8364	−73.7296	9/05/09	24.3	18.4	14.1 ± 0.8
RCK	Rocky Neck	CT	41.3006	−72.2379	13/09/10	30.3	19.2	49.1 ± 3.2
SBA	Sands Beach	NY	40.851	−73.7325	24/06/10	25.5	21.8	24.5 ± 2.8
SDP	Sands Point	NY	40.8649	−73.7009	24/06/10	25	20.4	21.0 ± 2.3
SRH	Shoreham	NY	40.967	−72.8538	16/06/09	25.3	15.8	20.2 ± 1.2
SIP	Sherwood Island State Park	CT	41.1113	−73.3344	14/09/10	28.2	20.8	40.3 ± 2.5
SLB	Smithtown, Long Beach	NY	40.9205	−73.1771	14/06/10	25.4	18.9	55.9 ± 5.9
SM	Sunken Meadow (aka SKN)	NY	40.9115	−73.2501	22/05/09	25.9	15.7	19.0 ± 1.2
SMT INT	Smithtown Inlet	NY	40.9051	−73.2309	29/05/09	19.3	15.1	44.5 ± 3.3
STB INT	Stony Brook Inlet	NY	40.9294	−73.1478	1/06/09	24.9	17.1	32.5 ± 1.5
STH	Southold	NY	41.0714	−72.4563	16/06/09	25.1	15.8	39.2 ± 1.2
STL	Stehli Beach, Oyster Bay	NY	40.9091	−73.5845	22/06/10	25.2	21.9	36.0 ± 4.0

(Continued)

Table 1. (Continued)

Station ID	Location	State	Latitude (N)	Longitude (W)	Date sampled	Salinity	Temperature (°C)	^{224}Ra (dpm 100 L^{-1})
Nearshore water								
WMB	West Meadow Beach	NY	40.9432	−73.1450	8/06/10	24.3	21.8	47.4 ± 5.1
WND	West Meadow	NY	40.9448	−73.1448	25/05/09	25.7	17.8	42.1 ± 3.0
WNR	West Neck Road, Huntington	NY	40.9067	−73.4836	22/07/10	26	25.6	33.9 ± 3.4
Pore water								
BV	Bayville	NY	40.9088	−73.5929	18/05/09	24.5	15.9	96.5 ± 6.3
LB	Smithtown, Long Beach	NY	40.9196	−73.1795	9/05/09	26	15.6	243.8 ± 15.6
SKN	Sunken Meadow	NY	40.9135	−73.2579	22/05/09	25.5	18.6	430.4 ± 87.2
SBA	Sands Beach Association	NY	40.851	−73.7325	24/06/10	25.1	22.1	223.8 ± 35.3
SDP	Sands Point Preserve	NY	40.8649	−73.7009	24/06/10	15.5	22	245.9 ± 47.9
NAV	Webb Institute of Naval Architecture	NY	40.8833	−73.6478	22/06/10	22.9	20.5	124.2 ± 24.7
STL	Stehli Beach, Oyster Bay	NY	40.9091	−73.5845	22/06/10	23.7	21.7	260.0 ± 51.9
WNR	West Neck Road, Huntington	NY	40.9067	−73.4836	22/07/10	25.5	26	310.0 ± 48.4
LYD	Lloyd Harbor, Huntington	NY	40.9153	−73.4512	22/07/10	21.4	28.2	317.6 ± 55.6
HBT	Hobart Beach	NY	40.9285	−73.4034	18/06/10	26	21.5	120.7 ± 23.6
CRM	Crab Meadow Beach	NY	40.9299	−73.3249	18/06/10	25.7	21.4	610.9 ± 120.0
SLB	Smithtown, Long Beach	NY	40.9205	−73.1771	14/06/10	25.1	18.6	289.3 ± 59.5
WMB	West Meadow Beach	NY	40.9432	−73.1450	8/06/10	25	21.6	677.8 ± 150.8
OFP	Old Field Point	NY	40.9771	−73.1196	10/06/10	24.9	20	412.3 ± 65.6
CDB	Cedar Beach	NY	40.9654	−73.0311	10/06/10	25.8	18.8	160.6 ± 31.2
SIP	Sherwood Island State Park	CT	41.1113	−73.3344	14/09/10	28.1	21.9	313.0 ± 44.3
LRD	Lordship Beach	CT	41.1475	−73.1294	14/09/10	27.9	21.8	408.1 ± 56.6
PCK	Peck Avenue, West Haven	CT	41.2585	−72.9402	14/09/10	27.4	23.2	378.0 ± 43.3
HRK	Harkness State Park	CT	41.3004	−72.1162	13/09/10	30.4	18.7	323.3 ± 38.8

found along the southern (New York) shore of LIS. Along the northern (Connecticut) shore of LIS, the activities of ^{224}Ra in beach pore waters ranged from 313 to 408 dpm 100 L^{-1}. The mean tidal range at these stations varied from 0.8 to 2.2 m, and ^{224}Ra pore-water activities along the shoreline were weakly and negatively correlated with the tidal range.

The transect made in Smithtown Bay from the shore out into the open LIS showed ^{224}Ra activities decreasing from approximately 71 dpm 100 L^{-1} at the shoreline to 15 dpm 100 L^{-1} 2 km from shore and decreasing further to between 5.0 and 4.6 dpm 100 L^{-1} in the open

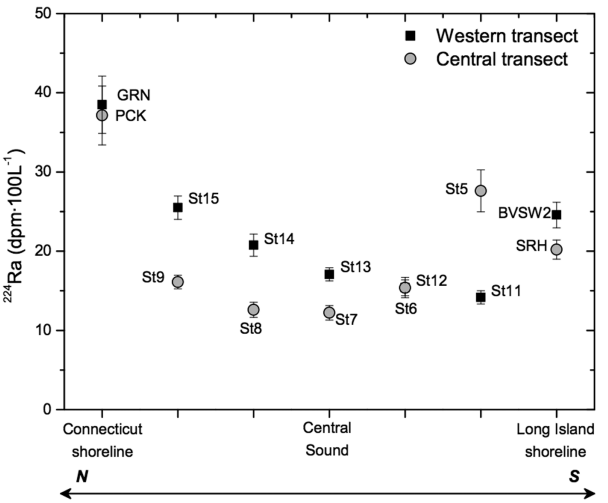

Figure 2. The ^{224}Ra concentrations for two transects across the sound. Stations are numbered as shown on the cross-sound transects in Figure 1 from Connecticut in the north (left) to Long Island (right) (from Garcia-Orellana et al. 2014). The concentration of ^{224}Ra in surface waters was 20.2 disintegrations per minute (dpm) 100 L^{-1} at the beach in Shoreham, New York (SRH) and 27.5 dpm 100 L^{-1} in the open water 2.2 km to the north (St5). BVSW2, Seawater sample #2, Bayville, New York; GRN, Greenwich, Connecticut; PCK, Peck Avenue, West Haven, Connecticut; St, station.

sound (Table 2). The ^{223}Ra decreased from 8.7 dpm 100 L^{-1} nearshore to between 0.4 and 0.6 dpm 100 L^{-1}in the open sound (Table 2). Salinity increased from 24.1 to 26.2 over the transect (Table 2). Although activities of both ^{223}Ra and ^{223}Ra decreased offshore, the ^{228}Ra and ^{226}Ra activities varied relatively little over distances from 10 to 2,000 m from shore (57 to 46 dpm 100 $L^{-1}$and 18.6 to 16.2 dpm 100 L^{-1},respectively; Fig. 4), although there is evidence of higher activities within 10 m of the shoreline (2 m sampling station; Table 2).

5. Discussion

a. Estimating residence times of beach pore water using ^{224}Ra

Our goal in this study is to use the short-lived radium isotopes to characterize drainage in beach sands. For this purpose, we adapt models that have been applied to advective transport of chemical species in groundwater. Applying a one-dimensional transport model to radium and neglecting hydrodynamic dispersion,

$$\frac{\partial C_{\mathrm{Ra}}}{\partial t} = -\upsilon \frac{\partial C_{\mathrm{Ra}}}{\partial x} + \frac{P}{(1+K)} - \lambda C_{\mathrm{Ra}}, \tag{1}$$

where C_{Ra} is the concentration of dissolved radium (atoms per volume of pore fluid), υ is the pore-water advective flow velocity (length per time), P is the rate of supply of radium atoms

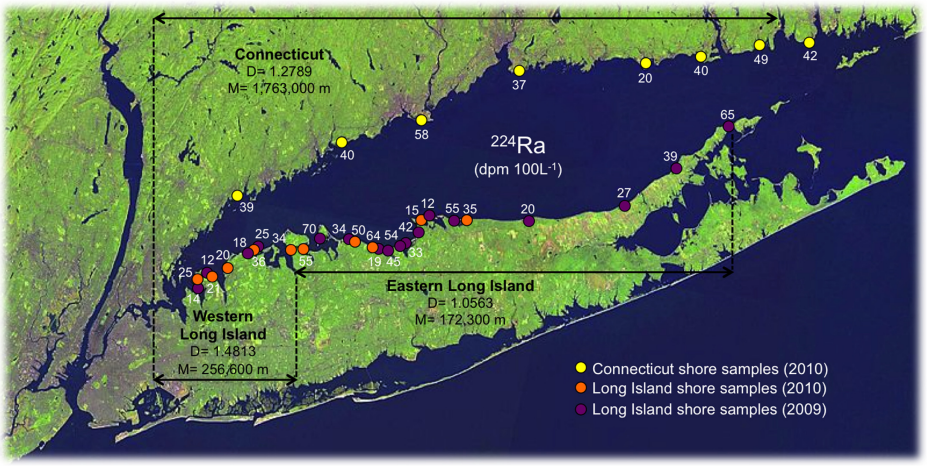

Figure 3. The ^{224}Ra concentrations (disintegrations per minute [dpm] 100 L^{-1}) in the open water along the shore of Long Island Sound. See Table 1 for station IDs. For later fractal analysis, the shoreline was divided into three sections. The "Connecticut" shore went from the Niantic River in the east westward to the Throgs Neck Bridge, New York. The eastern Long Island shore went from Orient Point, New York, in the east westward to Eatons Neck, New York. The western Long Island shore went from Eatons Neck to the Throgs Neck Bridge. The values for D and M refer to equation (5).

Table 2. Radium isotope data for Smithtown Bay transect (sampled June 2009). PW, porewater. SMT, Smithtown.

Station	Latitude (N)	Longitude (W)	Water depth (m)	Distance from shore (m)	Salinity	^{224}Ra	^{223}Ra	^{228}Ra	^{226}Ra
						(dpm 100 L^{-1})			
SMT PW	40.9183	−73.1853	0	0	25.5	174	18.9	95.6	25.2
SMT 1	40.9184	−73.1853	0.2	2	24.1	71.1	8.7	73.8	25.1
SMT 2	40.9184	−73.1853	0.5	10	24.1	60.3	8.0	57.4	18.6
SMT 3	40.9187	−73.1854	1	35	24.8	55.7	4.6	—	—
SMT 4	40.9192	−73.1855	1.2	100	25.7	30.6	2.4	41.8	15.5
SMT 5	40.9211	−73.1861	1.2	300	25.6	24.3	1.6	—	—
SMT 6	40.9249	−73.1872	5.2	750	26.0	16.9	0.8	53.1	17.8
SMT 7	40.9291	−73.1891	8.6	1, 250	25.8	16.0	0.9	—	—
SMT 8	40.9338	−73.1910	13.7	1, 750	25.7	13.2	1.1	43.9	13.8
SMT 9	40.9379	−73.1929	15	2, 250	25.9	15.4	1.0	—	—
SMT 10	40.9524	−73.1988	18.2	4, 000	25.7	5.8	0.5	46.2	16.2
SMT 11	40.9873	−73.2123	24.6	8, 000	25.9	4.6	0.4	—	—
SMT 12	41.0329	−73.2253	—	13, 000	26.2	5.0	0.6	—	—

Note: Dashes indicate not measured.

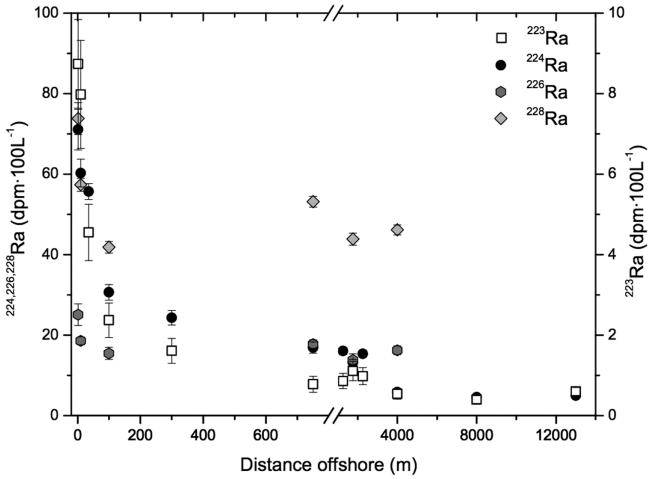

Figure 4. Radium concentrations along the transect in Smithtown Bay (see Figs. 1 and 5).

to the fluid phase, λ is the radium decay constant (1 per time), and K is a dimensionless sorption constant (disintegrations per minute radium on the solid per disintegrations per minute radium in solution).

Assuming steady state ($\partial C_{\mathrm{Ra}}/\partial t = 0$), equation (1) can be solved (Krest and Harvey 2003) as follows:

$$C_{\mathrm{Ra}} = P'\lambda^{-1} + [(c]^{o}_{\mathrm{Ra}} - P'\lambda^{-1})e^{-\frac{\lambda x}{\upsilon}} \tag{2}$$

where c^{o}_{Ra} is an initial radium concentration in the fluid and $P\prime = P/(1+K)$. Multiplying through by λ_{Ra} converts the atom concentrations to activities (disintegrations per minute per volume):

$$A_{\mathrm{Ra}} = P'\left(1 - e^{-\frac{\lambda x}{\upsilon}}\right) + A^{o}_{\mathrm{Ra}}e^{-\frac{\lambda x}{\upsilon}}. \tag{3}$$

Krest and Harvey (2003) applied equation (3) to detailed depth profiles of dissolved radium in a freshwater wetland (the Florida Everglades) in which flow was dominantly vertical. In the present case, we assume that water enters the beach sand with the radium activity measured immediately offshore and use that as the value of A^{o}_{Ra}. Moreover, we have sampled the beach pore water at only a single depth (~30 cm), and we further simplify equation (3) by replacing x/υ by a parameter we define as the residence time of the pore water (T). The modified equation

$$A_{\mathrm{Ra}} = P'\left(1 - e^{-\lambda T}\right) + A^{o}_{\mathrm{Ra}}e^{-\lambda T} \tag{4}$$

treats the dissolved radium in every parcel of water sampled as representing a balance between supply of radium to the pore water and loss by decay and advection.

Evaluating the term P' in equation (4) is crucial to the calculation of pore-water residence times. The short-lived radium isotopes ^{223}Ra and ^{224}Ra enter sediment pore water principally through recoil after their production from decay of their parent nuclides, ^{227}Th and ^{228}Th, in the solid phase. Once in the pore water, their dissolved activities are controlled by radioactive decay, sorption onto the solid surfaces, and any loss due to advection. We measured the value of P' at Smithtown beach directly by incubating a single core from Smithtown Bay beach with its pore water for several weeks, long enough for ^{224}Ra to reach a steady state between production, decay, and sorption. The ^{224}Ra activities in the pore water of the beach sand at steady state reached 1,102 $\pm$ 62 dpm 100 L^{-1}. Using this value of P in equation (4), we can estimate the residence time of the samples taken at the beach in Smithtown Bay (SLB in Table 1). The activity of ^{224}Ra in water entering the sediment at high tide in (June 2010; taken as A^o_{Ra}) was 56 $\pm$ 6 dpm 100 L^{-1}, whereas it was 289 $\pm$ 60 dpm 100 L^{-1} in the shallow pore water of the beach sand. The residence time of the shallow beach pore water calculated from equation (4) is 1.3 d. Pore-water ^{224}Ra activities also were measured at Smithtown beach in June 2009, when the transect samples were collected (71 dpm 100 L^{-1} for the incoming water and 174 dpm 100 L^{-1}for the pore water; Table 2). The measured activities yielded a residence time of 0.6 d. We do not have measurements of long-term steady-state ^{224}Ra activities (P) at the other shore sites, but assuming they are comparable to that at Smithtown beach (i.e., $\sim$1,100 dpm 100 L^{-1}), the longest residence time is approximately 2.5 d (based on the offshore and pore-water ^{224}Ra activities at Sunken Meadow; SKN in Table 1). These results suggest that the flux of water through the shallow beach face can be variable spatially and temporally, but that the shallow pore water has a relatively short residence time at all the sites sampled. A tentative negative correlation with the tidal range suggests to us that a larger tidal range tends to reduce the residence time.

The simple model of equation (4) includes only one external input of radium to the shallow beach pore water—namely, infiltration of offshore water input into the intertidal beach—but the pore water may also include deeper, marine groundwater as a mixing end member. Pore-water activities of the long-lived ^{226}Ra may help to ascertain whether such mixing is taking place because its half-life is so long that significant amounts would not be recoiled to sediment pore water over the residence times indicated from ^{224}Ra. Thus, elevated activities of ^{226}Ra in the beach pore water would indicate such mixing. We measured ^{226,228}Ra data in a beach pore-water sample obtained during the transect sampling of Smithtown Bay (Table 2). The pore-water ^{226}Ra activity (25.2 dpm 100 L^{-1}) is identical to that measured in the shallow water sampled 2 m from shore, but somewhat greater than the activities over the transect in the bay (Table 2). The ^{228}Ra shows some enrichment in the beach pore water relative to the water immediately offshore (Table 2), but also little gradient beyond 10 m from shore. If deeper groundwater is entering the surficial beach zone and becomes a part of the discharge we document from the beach, then equation (4) could be modified to factor in an additional value of A^o_{Ra}. Such a modification would likely decrease the calculated residence times. Additional measurements of the radium isotopes at depth in the beach sands would help to evaluate the possibility more thoroughly.

The range of pore-water ^{224}Ra activities (and residence times calculated from them) found in the various beaches most likely represents different travel times of the water sampled and, possibly, varying grain sizes of the beach sands and differences in the beach slopes and tidal ranges. Although all samples were collected near the low-tide shoreline, the path by which pore water reached that location may have been deeper in some cases and shallower in others. Longer residence times would result in higher pore-water ^{224}Ra activities up to the equilibrium or steady-state values. The samples were taken in the shallowest part of the upper saline plume; longer residence times, and higher radium concentrations, would be expected deeper in the beach. In either situation, the flux of ^{224}Ra from the intertidal beach can be identified as an important contributor to the elevated concentrations of ^{224}Ra observed at the nearshore stations.

b. The ^{224}Ra flux to Smithtown Bay from the intertidal zone

The gradient in ^{224}Ra from the beach into Smithtown Bay indicates an SGD that we have ascribed to circulation of seawater through the intertidal beach face. In this situation, the geometry of the shoreline, as well as the density structure of the nearshore water column, would influence the observed ^{224}Ra concentrations nearshore. Interpretation of geotracer data of this sort is often done on individual transects assuming a linear shoreline. However, if the shoreline is curvilinear, the interpretation of radial transects becomes confounded by the angular dependence of the shoreline sources. In the case of Smithtown Bay, the beach provides ^{224}Ra from the intertidal zone along a concave shoreline. In order to estimate the ^{224}Ra source and SGD per meter of shoreline, the curvature of the shoreline was incorporated numerically by the volume represented in empirical, coastal cells (Fig. 5). Multiplying the ^{224}Ra inventories measured at each station by the volume they represent, a total ^{224}Ra inventory of 2.5×10^6 dpm m^{-1} was calculated. If we assume that this inventory was in steady state, the flux required to support it was obtained by multiplying the inventory by λ_{224} (0.190 d^{-1}). The resultant value was 4.90×10^5 dpm m^{-1} d^{-1}, or an annual flux of 1.79×10^8 dpm m^{-1} y^{-1}.

c. Supply of ^{224}Ra to LIS via circulation through the intertidal zone

Our data support a flux of ^{224}Ra to Smithtown Bay via SGD due to the circulation of seawater through the beach sand in the intertidal zone. Given the nature of the shorelines of LIS, this process is likely an important source of ^{224}Ra to the sound as a whole. In an attempt to calculate the total intertidal flux of radium, or SGD, to LIS, we extrapolated values per meter of Smithtown Bay shoreline to the entire coastline of the sound. The length of Long Island's shoreline, however, can be an elusive number. The tortuosity or irregularity of shorelines is relevant to the description of coastal processes. All travelers recognize the important distinction between distances "as the crow flies" and the actual length of the same journey on the ground with all its dimensions. More than 60 years ago, Steinhaus (1954, p. 8, as cited in Mandelbrot 1967) noticed that "the left bank of the Vistula, when measured

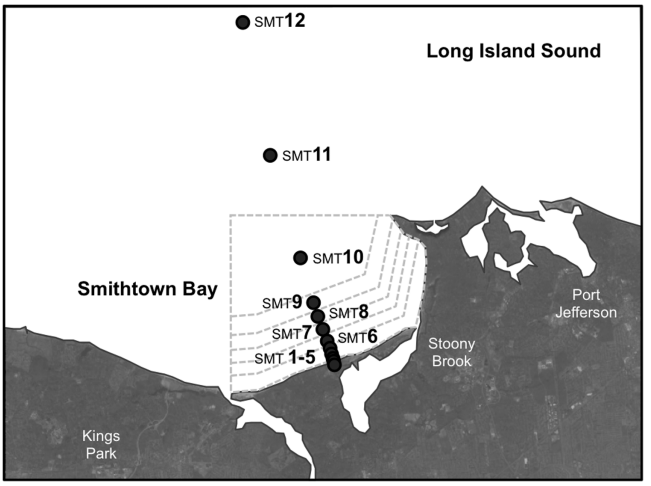

Figure 5. Geometry of Smithtown Bay relative to sample locations. Empirical, coastal cells are represented by dotted lines. SMT, Smithtown.

with increased precision would furnish lengths ten, hundred or even thousand times as great as the length read off a school map." Empirical observations show that the measured length of a coastline increases as smaller and smaller features are taken into account (Richardson 1961, as cited in Mandelbrot 1967). The fractal dimension is a number between 1 and 2. More contorted shorelines have higher fractal dimensions. The smooth coast of South Africa, for example, has a fractal dimension of 1.02, whereas the more irregular coast of Britain is 1.25 (Mandelbrot 1967). In general, the shoreline length is

$$L(s) = M(s)^{(1-D)}, \tag{5}$$

where L is the shoreline length as a function of step size, s is the size of the step used to measure the length, M is an empirical constant, and D is the fractal dimension (Mandelbrot 1967). Measurements were made on a 1:80,000 chart of LIS by setting a pair of dividers to correspond to various distances in turn, walking the dividers around the map's shoreline, and counting the number of steps needed to complete a full circuit of LIS. Given the geological character of the shoreline, however, it was divided into three sections (Fig. 3). The rocky shoreline of Connecticut (and Westchester County in New York), from the Niantic River to the Throgs Neck Bridge, had $D = 1.2789 (M = 1{,}762{,}788$ m); the eastern Long Island shore, from Orient Point to Eatons Neck, had $D = 1.0563 (M = 172{,}306$ m); and the western, embayed Long Island shore, from Eatons Neck to the Throgs Neck Bridge, had $D = 1.4183 (M = 256{,}625$ m). The shoreline length of LIS as a function of step size is shown in Figure 6.

Values of the shoreline length are quite high for small step sizes, but, for this intertidal process, we might expect the appropriate step size to be fairly small. Most of the inventory

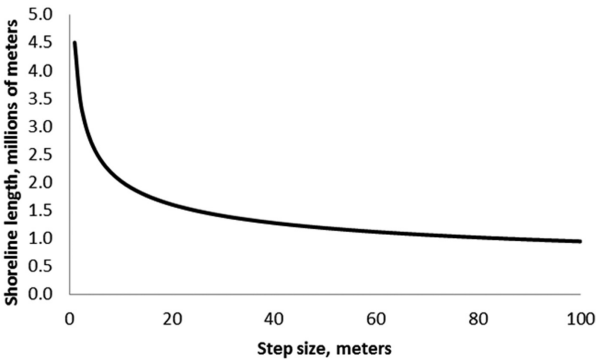

Figure 6. Fractal shoreline length versus step size for the entire shoreline of Long Island Sound.

of ^{224}Ra derived from intertidal circulation might be expected to be contained within a zone approximately 100 m wide (Fig. 4). For a step size between 50 and 500 m, the entire shoreline of LIS would be between 11.9×10^5 and 5.7×10^5 m, respectively. The shoreline ^{224}Ra input calculated for Smithtown Bay was 1.79×10^8 dpm m^{-1} y^{-1}. Extrapolating this flux to shoreline lengths of the Long Island shoreline for step sizes of between 50 and 500 m yields ^{224}Ra inputs of between 213×10^{12} and 102×10^{12} dpm y^{-1}, respectively. These values are comparable to the SGD term determined by Garcia-Orellana et al. (2014) from a ^{224}Ra balance in the main body of the sound, which was calculated to be between 106×10^{12} and 244×10^{12} dpm y^{-1}, depending on the season.

The average end-member concentration of ^{224}Ra in the pore-water of Long Island beaches was approximately 313 dpm 100 L^{-1}. Applying this value to the fluxes calculated previously yields volumetric fluxes of between 6.6×10^{10} and 3.1×10^{10} m^3 y^{-1}. (In Smithtown Bay, this corresponds to an SGD input of between 188 and 1,203 m^3 m^{-1} d^{-1} whereas the direct inventory (section 5b) yields 160 m^3 m^{-1} d^{-1}). In comparison, the amount of fresh groundwater flowing under the shoreline through the coastal aquifer in Nassau and Suffolk counties had been estimated from a groundwater-flow model to be 0.034×10^{10} m^3 y^{-1} (Monti and Scorca 2003). Much if not most of the fresh groundwater would be expected to discharge near the coast. Around Smithtown Bay, the fresh groundwater would be discharged into the bay proper, although some would be entering a coastal embayment, Stony Brook Harbor. Regardless of the injection site, the freshwater component of the total SGD would be equivalent to 1%, or less, of the circulated sound-water component. In other words, circulated seawater accounted for more than 99% of the SGD into LIS.

d. Biogeochemical consequences of tidally recirculated SGD

The large gradient in ^{224}Ra away from shore and the short residence times calculated for the pore water of the beach sands imply that circulation and mixing is rapid through this zone. It seems likely that under these circumstances the behavior of other chemical elements, such

as silicon or barium, or long-lived radionuclides, such as ^{238}U, is not affected, depending on their reaction rates in the pore water of the beach sands. In contrast, organic matter infiltrated into the shallow beach sands by the tides and wave swash may be remineralized rapidly, and the flux of dissolved nutrients to the nearshore waters via tidally modulated SGD may be substantial. Additional data on nutrient concentrations in the pore waters and offshore waters are needed to evaluate this possibility. Deeper groundwater, for example in the coastal aquifer under the beach face, may represent a more active geochemical system for metals such as iron and manganese, especially if oxic surficial waters mix with suboxic groundwater (Charette and Sholkovitz 2006; Beck, Cochran, and Sañudo-Wilhelmy 2010). However, the lack of nearshore enrichments in the long-lived ^{226}Ra supports the notion that processes operating deeper in the coastal aquifer are not affecting the shallow surface waters offshore in LIS.

6. Conclusions

SGD is often much greater than the seepage of fresh groundwater under the shoreline (Reilly and Goodman 1985; Cartwright, Li, and Nielsen 2004; Mulligan and Charette 2006). Li et al. (1999) report that 90% or more of SGD might be composed of circulated seawater. SGD from the intertidal zone along LIS margins is a major contributor of both SGD and ^{224}Ra to LIS, and circulated seawater accounts for more than 99% of the volumetric SGD flux. Similar contributions should be expected at other mesotidal sites with intertidal beaches composed of permeable sands. Both the curvature of the shoreline and the relevant size of the shoreline length (step size) must be taken into account when extrapolating measurements.

Acknowledgments. This project has been funded by New York Sea Grant (Project R/CCP-16) and the Spanish Government (CTM2010-11232-E), and we greatly appreciate their support. JG-O was also fortunate to have support from the government of Spain and the Fulbright Commission for a postdoctoral fellowship (ref. 2007-0516) and the Generalitat de Catalunya to Marine and Environmental Biogeosciences Research Group (2014 SGR-1356). VR gratefully acknowledges financial support through a PhD fellowship (AP2008-03044) from MICINN (Spain). We thank David Bowman and the crews of the R/V *Seawolf* for their assistance in sampling, Professor Robert Aller for helpful discussions, and the anonymous reviewers for their advice and guidance.

REFERENCES

Abarca, E., H. Karam, H. F. Hemond, and C. F. Harvey. 2013. Transient groundwater dynamics in a coastal aquifer: The effects of tides, the lunar cycle, and the beach profile. Water Resour. Res., *49*, 2473–2488.

Anschutz, P., T. Smith, A. Mouret, J. Deborde, S. Bujan, D. Poirier, and P. Lecroart. 2009. Tidal sands as biogeochemical reactors. Estuarine, Coastal Shelf Sci., *84*, 84–90.

Austin, M. J., and G. Masselink. 2006. Swash–groundwater interaction on a steep gravel beach. Cont. Shelf Res., *26*, 2503–2519.

Bauer, C. L. 2012. Physical Processes Contributing to Localized, Seasonal Hypoxic Conditions in the Bottom Waters of Smithtown Bay, Long Island Sound, New York. MS thesis. Stony Brook, NY: School of Marine and Atmospheric Sciences, State University of New York at Stony Brook, 112 pp.

Beck, A. J., J. K. Cochran, and S. A. Sañudo-Wilhelmy. 2010. The distribution and speciation of dissolved trace metals in a shallow subterranean estuary. Mar. Chem., *121*, 145–156.

Boehm, A. B., A. Paytan, G. G. Shellenbarger, and K. A. Davis. 2006. Composition and flux of groundwater from a California beach aquifer: Implications for nutrient supply to the surf zone. Cont. Shelf Res., *26*, 269–282.

Bowman, M. J., and W. E. Esaias. 1977. Coastal jets, fronts, and phytoplankton patchiness. Elsevier Oceanogr. Ser., *19*, 255–268.

Brovelli, A., X. Mao, and D. A. Barry. 2007. Numerical modeling of tidal influence on density-dependent contaminant transport. Water Resour. Res.,43. doi: 10.1029/2006WR005173

Burnett, W. C., H. Bokuniewicz, M. Huettel, W. S. Moore, and M. Taniguchi. 2003. Groundwater and pore water inputs to the coastal zone. Biogeochemistry, *66*, 3–33.

Cartwright, N., L. Li, and P. Nielsen. 2004. Response of the salt–freshwater interface in a coastal aquifer to a wave-induced groundwater pulse: Field observations and modelling. Adv. Water Resour., *27*, 297–303.

Charette, M. A., and E. R. Sholkovitz. 2006. Trace element cycling in a subterranean estuary: Part 2. Geochemistry of the pore water. Geochim. Cosmochim. Acta, *70*, 811–826.

Connecticut Department of Environmental Protection. 2010. Long Island Sound Hypoxia Season Review. Hartford, CT: Connecticut Department of Environmental Protection.

Davies, D. S., E. W. Axelrod, and J. S. O'Connor. 1972. Erosion of the North Shore of Long Island. Technical Report 18. Stony Brook, NY: Marine Sciences Research Center, State University of New York, 101 pp.

Deborde, J., P. Anschutz, I. Auby, C. Glé, M.-V. Commarieu, D. Maurer, P. Lecroart, and G. Abril. 2008. Role of tidal pumping ion nutrient cycling in a temperate lagoon (Arcachon Bay, France). Mar. Chem., *109*, 98–114.

Garcia-Orellana, J., J. K. Cochran, H. Bokuniewicz, J. W. R. Daniel, V. Rodellas, and C. Heilbrun. 2014. Evaluation of ^{224}Ra as a tracer for submarine groundwater discharge in Long Island Sound (NY). Geochim. Cosmochim. Acta, *141*, 314–330.

Garcia-Orellana, J., V. Rodellas, N. Casacuberta, E. Lopez-Castillo, M. Vilarrasa, V. Moreno, E. Garcia-Solsona, and P. Masqué. 2013. Submarine groundwater discharge: Natural radioactivity accumulation in a wetland ecosystem. Mar. Chem., *156*, 61–72.

Garcia-Solsona E., J, Garcia-Orellana, P. Masqué, and H. Dulaiova. 2008. Uncertainties associated with ^{223}Ra and ^{224}Ra measurements in water via a delayed coincidence counter (RaDeCC). Mar. Chem., *109*, 198–219.

Hays, R. L., and W. J. Ullman. 2007. Dissolved nutrient fluxes through a sandy estuarine beachface (Cape Henlopen, Delaware, U.S.A.): Contributions from fresh groundwater discharge, seawater recycling, and diagenesis. Estuaries Coasts, *30*, 710–724.

Krest, J. M., and J. W. Harvey. 2003. Using natural distributions of short-lived radium isotopes to quantify groundwater discharge and recharge. Limnol. Oceanogr., *48*, 290–298.

Krest J. M., W. S. Moore, L. R. Gardner, and J. T. Morris. 2000. Marsh nutrient export supplied by groundwater discharge: Evidence from radium measurements. Global Biogeochem. Cycles, *14*, 167–176.

Li, L., D. A. Barry, F. Stagnitti, and J.-Y. Parlange. 1999. Submarine groundwater discharge and associated chemical input to a coastal sea. Water Resour. Res., *35*, 3253–3259.

Loveless, A. M., and C. E. Oldham. 2010. Natural attenuation of nitrogen in groundwater discharging through a sandy beach. Biogeochemistry, *98*, 75–87.

Mandelbrot, B. B. 1967. How long is the coast of Britain? Statistical self-similarity and fractional dimension. Science, *156*, 636–638.

Monti, J., Jr., and M. P. Scorca. 2003. Trends in Nitrogen Concentration and Nitrogen Loads Entering the South Shore Estuary Reserve from Streams and Ground-Water Discharge in Nassau and Suffolk Counties, Long Island, New York, 1952-97. Water-Resources Investigations Report 02-4255. Coram, NY: U.S. Geological Survey, 36 pp.

Moore, W. S., and R. Arnold. 1996. Measurement of ^{223}Ra and ^{224}Ra in coastal waters using a delayed coincidence counter. J. Geophys. Res.: Oceans, *101*, 1321–1329.

Mulligan, A. E., and M. A. Charette. 2006. Intercomparison of submarine groundwater discharge estimates from a sandy unconfined aquifer. *J. Hydrol.*, *327*, 411–425.

Rapaglia, J. P., and H. J. Bokuniewicz. 2009. The effect of groundwater advection on salinity in pore waters of permeable sediments. Limnol. Oceanogr., *54*, 630–643.

Reilly, T. E., and A. S. Goodman. 1985. Quantitative analysis of saltwater-freshwater relationships in groundwater systems—a historical perspective. J. Hydrol., *80*, 125–160.

Richardson, L. F. 1961. The problem of contiguity: An appendix to statistics of deadly quarrels. Gen. Syst. Yearb., *6*, 139.

Robinson, C., L. Li, and D. A. Barry. 2007. Effect of tidal forcing on a subterranean estuary. Adv. Water Resour., *30*, 851–865.

Santos, I. R., W. C. Burnett, T. Dittmar, I. G. N. A. Suryaputra, and J. Chanton. 2009. Tidal pumping drives nutrient and dissolved organic matter dynamics in a Gulf of Mexico subterranean estuary. Geochim. Cosmochim. Acta, *73*, 1325–1339.

Slomp, C. P., and P. Van Cappellen. 2004. Nutrient inputs to the coastal ocean through submarine groundwater discharge: Controls and potential impact. J. Hydrol., *295*, 64–86.

Smith, A. J. 2004. Mixed convection and density-dependent seawater circulation in coastal aquifers. Water Resour. Res., *40*. doi: 10.1029/2003WR002977

Steinhaus, H. 1954. Length, shape and area. Colloq. Math., *3*, 1–13.

Taniguchi, M., W .C. Burnett, J. E. Cable, and J. V. Turner. 2002. Investigation of submarine groundwater discharge. Hydrol. Processes, *16*, 2115–2129.

Torgersen, T., K. K. Turekian, V. C. Turekian, N. Tanaka, E. DeAngelo, and J. O'Donnell. 1996. ^{224}Ra distribution in surface and deep water of Long Island Sound: Sources and horizontal transport rates. Cont. Shelf Res., *16*, 1545–1559.

Turner, I. L., and G. Masselink. 1998. Swash infiltration-exfiltration and sediment transport. J. Geophys. Res.: Oceans, *103*, 30813–30824.

Ullman, W. J., B. Chang, D. C. Miller, and J. A. Madsen. 2003. Groundwater mixing, nutrient diagenesis, and discharge across a sandy beachface, Cape Henlopen, Delaware (USA). Estuarine, Coastal Shelf Sci., *57*, 539–552.

Urish, D. W., and T. E. McKenna. 2004. Tidal effects on ground water discharge through a sandy marine beach. Groundwater, *42*, 971–982.

Valiela, I., J. Costa, K. Foreman, J. M. Teal, B. Howes, and D. Aubrey. 1990. Transport of groundwater-borne nutrients from watersheds and their effects on coastal waters. Biogeochemistry, *10*, 177–197.

Vandenbohede, A., and L. Lebbe. 2006. Occurrence of salt water above fresh water in dynamic equilibrium in a coastal groundwater flow system near De Panne, Belgium. Hydrogeol. J., *14*, 462–472.

Welsh, B. L., and F. C. Eller. 1991. Mechanisms controlling summertime oxygen depletion in western Long Island Sound. Estuaries, *14*(3), 265–278.

Windom, H. L., W. S. Moore, L. F. H. Niencheski, and R. A. Jahnke. 2006. Submarine groundwater discharge: A large, previously unrecognized source of dissolved iron to the South Atlantic Ocean. Mar. Chem., *102*, 252–266.

Xin, P., C. Robinson, L. Li, D. A. Barry, and R. Bakhtyar. 2010. Effects of wave forcing on a subterranean estuary. Water Resour. Res., *46*, W12505. doi: 10.1029/2010WR009632

Received: *6 January 2014*; revised: *2 June 2015*.